Environmental Science & Technology

pubs.acs.org/est

Article

Stable Sulfur Isotopes Revealed a Major Role of Transition-Metal Ion-Catalyzed SO_2 Oxidation in Haze Episodes

Jianghanyang Li, Yan-Lin Zhang,* Fang Cao, Wenqi Zhang, Meiyi Fan, Xuhui Lee, and Greg Michalski

Cite This: *Environ. Sci. Technol.* 2020, 54, 2626−2634

Read Online

ACCESS | Metrics & More | Article Recommendations

ABSTRACT: Secondary sulfate aerosols played an important role in aerosol formation and aging processes, especially during haze episodes in China. Secondary sulfate was formed via atmospheric oxidation of SO_2 by OH, O_3, H_2O_2, and transition-metal-catalyzed (TMI) O_2. However, the relative importance of these oxidants in haze episodes was strongly debated. Here, we use stable sulfur isotopes ($\delta^{34}S$) of sulfate aerosols and a Rayleigh distillation model to quantify the contributions of each oxidant during a haze episode in Nanjing, a megacity in China. The observed $\delta^{34}S$ values of sulfate aerosols showed a negative correlation with sulfur oxidation ratios, which was attributed to the sulfur isotopic fractionations during the sulfate formation processes. Using the average fractionation factor calculated from our observations and zero-dimensional (0-D) atmospheric chemistry modeling estimations, we suggest that OH oxidation was trivial during the haze episode, while the TMI pathway contributed 49 ± 10% of the total sulfate production and O_3/H_2O_2 oxidations accounted for the rest. Our results displayed good agreement with several atmospheric chemistry models that carry aqueous and heterogeneous TMI oxidation pathways, suggesting the role of the TMI pathway was significant during haze episodes.

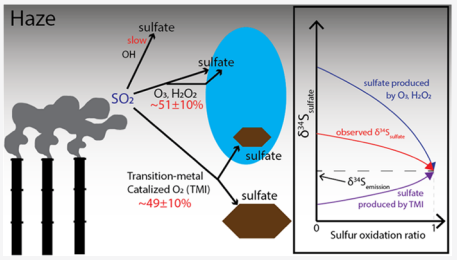

INTRODUCTION

Haze episodes in Chinese cities are adversely affecting the environment and the health of millions of residents. Most haze episodes are characterized by high concentrations and fast accumulation of aerosol sulfate,[1−4] which could contribute to as much as 45% of the total aerosol mass. Over 90% sulfate in haze episodes is the secondary sulfate, i.e., the sulfate produced from SO_2 oxidation in the atmosphere via (1) gas-phase oxidation by OH radical;[5] (2) aqueous oxidation by H_2O_2, O_3, and transition-metal ion (TMI)-catalyzed O_2;[6−12] and (3) heterogeneous oxidation on the surface of aerosols, cloud droplets, and mineral dusts by the same oxidants as aqueous oxidation.[1,13−16] Some studies[11,12,14,17,18] also suggested that NO_2 might play an important role during the formation of the aerosol sulfate, probably by facilitating TMI oxidation,[19] which is based on an experimental study[20] that demonstrated that the direct oxidation of SO_2 by NO_2 was several orders of magnitude slower than gas-phase OH oxidation. However, aerosol collected from several Chinese urban areas (e.g., Nanjing) was acidic,[21] suggesting that NO_2 oxidation might not be important in these regions. Furthermore, a recent GEOS-Chem modeling study[22] has suggested that NO_2 oxidation contributed less than 2% of total sulfate production during haze episodes. While the gas-phase oxidation rate of SO_2 + OH is well-constrained, there are many uncertainties in quantifying the rates of aqueous and heterogeneous SO_2 oxidation. One of the ongoing debates is the relative contribution of each SO_2 oxidation pathway during haze episodes. Some[8,12,13] have suggested that O_3 and H_2O_2 oxidation of SO_2 in the aqueous phase contributed to the majority of total sulfate production, while the TMI pathway played a minor role. Others[17,23] have countered that the TMI pathway is likely also very important in highly polluted regions. Therefore, addressing this debate is essential to unravel the complex atmospheric sulfur chemistry in haze episodes.

Atmospheric chemistry models are often used to study the sulfate chemistry, but many models have uncertainties in parameterizing aqueous and heterogeneous SO_2 oxidation chemistry under haze conditions, resulting in underestimation of sulfate formation rates during haze episodes.[1,24−26] One of the biggest uncertainties is the pH of aerosol water; several studies had attempted to calculate the aerosol water pH in Beijing[12,17,27−29] using the same model (ISORROPIA II). Depending on assumptions about whether the aqueous phase is at the thermodynamic stable state,[17,30] the calculated pH was either 3−5 or >5.5. This uncertainty greatly impacts the quantification of the aqueous SO_2 oxidation rate.[31] A pH increase of 1 unit will increase the O_3 oxidation rate by 2 orders of magnitude but decrease the TMI oxidation rate by 2−3 orders of magnitude. Conversely, the rate of SO_2 oxidation by H_2O_2 is insensitive to the changing pH. Additionally, atmospheric models usually quantify the rate of

Received: November 25, 2019
Revised: January 13, 2020
Accepted: January 16, 2020
Published: January 16, 2020

the TMI oxidation pathway using modeled aerosol Fe and Mn concentrations.[10] However, studies[9,32] have suggested that aerosol surface type, temperature, irradiation, and the existence of other transition metals in aerosol water could alter the rate of TMI oxidation by as much as 2 orders of magnitude, adding more complexity to this question. Therefore, to (1) reduce the uncertainties in atmospheric models and (2) verify the performance in models during haze episodes, an alternative approach is needed to assess the relative importance of each oxidation pathway.

The isotopic composition of sulfate aerosols has been used to determine the formation processes of sulfate aerosols. The mass-independent fractionation signals (nonzero $\Delta^{17}O$, where $\Delta^{17}O = \delta^{18}O - 0.52 \times \delta^{17}O$) of oxygen isotopes in sulfates are often used to estimate the contributions of $SO_2 + O_3$ and H_2O_2 to the formation of sulfate aerosols,[10,17,33] since $SO_2 + O_3$ and $SO_2 + H_2O_2$ are the only known two pathways that produce nonzero $\Delta^{17}O$ values in sulfates.[34] The sulfate formed via $SO_2 + O_3$ yields $\Delta^{17}O = 6.5‰$, and the sulfate formed via $SO_2 + H_2O_2$ shows $\Delta^{17}O = 0.7‰$. This method can easily identify the significant contribution of the $SO_2 + O_3$ pathway when high $\Delta^{17}O$ (>3‰) is measured in sulfate samples. There is significant uncertainty, however, when interpreting sulfate aerosols with low $\Delta^{17}O$ values (<1‰). Unfortunately, most sulfate aerosols in haze episodes show $\Delta^{17}O < 1‰$,[17,22] suggesting a limited contribution from the $SO_2 + O_3$ pathway but the relative importance of the $SO_2 + H_2O_2$ pathway and the TMI pathway is still unclear. Therefore, solely using $\Delta^{17}O$ probably cannot precisely distinguish the contributions from the $SO_2 + H_2O_2$ and the TMI pathways in haze episodes.

Stable sulfur isotopes ($\delta^{34}S$) have the potential to indicate the formation pathways of sulfate aerosols. The fractionation factors for sulfur isotopes during multiple oxidation pathways (SO_2 + OH, $SO_2 + H_2O_2/O_3$, and TMI) have been determined experimentally.[35−37] Yet, to date, there are few studies using sulfate $\delta^{34}S$ values to interpret the oxidation pathways of SO_2.[35,38,39] This is because the $\delta^{34}S$ values of sulfate aerosols ($\delta^{34}S_{sulfate}$) are simultaneously controlled by the $\delta^{34}S$ values of SO_2 sources[40,41] ($\delta^{34}S_{emission}$) and the kinetic and equilibrium isotope effects occurring during the oxidation process. The $\delta^{34}S_{emission}$ values strongly depend on the origin of SO_2 and can, therefore, be difficult to constrain. However, during haze episodes, SO_2 generally originates from local sources because air stagnation limits long-range transport and the $\delta^{34}S_{emission}$ values can be well-constrained using local SO_2 emission inventory and observations. Thus, the differences between $\delta^{34}S_{emission}$ and $\delta^{34}S_{sulfate}$ can be attributed to the isotopic fractionations during the oxidation processes, which are controlled by the oxidation pathways. This isotopic fractionation during SO_2 oxidation should be treated as a Rayleigh distillation process[42] since isotopic exchange between the product sulfate and the reactant SO_2 is minimal.[35] Currently, many studies have measured $\delta^{34}S_{sulfate}$ in Chinese megacities[38,39,43−47] to understand the sources of atmospheric SO_2 and the secondary sulfate aerosols. Some works also have measured $\delta^{33}S$ and $\delta^{36}S$[47−51] to further constrain the origins of atmospheric SO_2. However, the differences between $\delta^{34}S_{emission}$ and $\delta^{34}S_{sulfate}$, as well as the isotopic fractionation process during the formation of sulfate, were rarely discussed and poorly understood. Here, we used the Rayleigh distillation model to investigate the sulfur isotopic fractionations of sulfate aerosols collected during a haze episode in winter 2015 at Nanjing, China, to understand the relative contribution of each SO_2 oxidation pathway.

MATERIALS AND METHODS

Sulfate aerosols were sampled during a severe haze episode in winter 2015, in Nanjing, People's Republic of China. The sampling site was located at the Agrometeorological station in Nanjing University of Information Science and Technology (NUIST). Two large industrial areas are located ∼10 km northeast and ∼5 km southwest of the sampling site, and downtown Nanjing is 20 km to the southeast (Figure 1). A high-volume aerosol sampler equipped with a precombusted quartz filter was used to collect ambient aerosol samples (<2.5 μm in diameter, $PM_{2.5}$) from January 22nd to 28th at a flow rate of 1 m^3/min, and the filter was replaced every 3 h. Once the aerosol samples were collected, the filters were wrapped in an aluminum foil, sealed in air-tight polyethylene bags, and stored in a freezer to minimize sample loss or evaporation. To determine the anion and cation concentrations of filter samples, a quarter of each filter was cut and the soluble components on the filter were dissolved into 50 mL of Millipore water (18.2 MΩ). Then, the solution was sonicated for at least 30 min to ensure all of the soluble ions were completely dissolved. Subsequently, the solutions were filtered through 0.45 μm filters to remove insoluble materials. An aliquot of each solution was taken and was used to measure the anion and cation concentrations using a Dionex ICS 5000+ at NUIST following the standard ion chromatography (IC) procedure,[52] while the rest of the solutions were kept frozen. The analytical uncertainty for the IC analysis was ±5%. Meteorological data (wind speed and direction, temperature, and RH) were obtained from an automatic meteorological station next to the sampling site. Concentrations of pollutants ($PM_{2.5}$, NO, NO_2, O_3, CO, and SO_2) were obtained from the environmental supervising station at Pukou District, Nanjing, ∼15 km away from the sampling site.

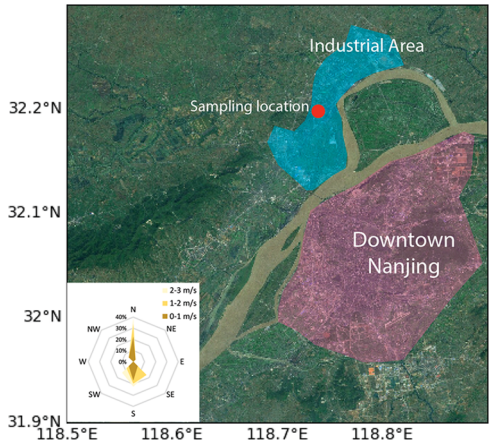

Figure 1. Sampling location was in between two large industrial areas (blue) and downtown Nanjing (red) is 20 km to the southeast. Wind rose during the sampling period is shown at the lower-left corner; the highest 3 h wind speed was <3 m/s, indicating air stagnation.

The sulfur isotopic analysis was conducted at the Purdue Stable Isotope Laboratory at the Purdue University. The sulfur isotopic analysis follows the procedure by Li et al.[40] Another quarter of each sample was again dissolved into 10 mL of Millipore water (18.2 MΩ), and each solution was sonicated

https://dx.doi.org/10.1021/acs.est.9b07150
Environ. Sci. Technol. 2020, 54, 2626−2634

for 30 min to completely dissolve all of the sulfates on the filter. To completely precipitate $BaSO_4$, 1 mL of 5% $BaCl_2$ solution and subsequently 0.5 mL of 37% HCl were added into each sample solution. Between 0.1 and 0.5 mg of the $BaSO_4$ precipitate was then weighed into tin boats and combusted at 980 °C in an elemental analyzer (Costec), and then the product SO_2 was directed into an isotope ratio mass spectrometer (ThermoDeltaV) to measure the $\delta^{34}S$ values. The analytical uncertainty of the sulfur isotopic analysis was ±0.1‰, inferred from IAEA-SO5 and IAEA-SO6 external standards.

RESULTS AND DISCUSSION

The haze episode occurred in Nanjing during winter 2015 and was characterized by high $PM_{2.5}$, high sulfate concentrations, and air stagnation. Prior to the haze episode (between January 18 and 21, 2015), the $PM_{2.5}$ concentrations averaged 83.1 $\mu g/m^3$. The haze episode began between January 22, 00:00 and January 23, 12:00 when $PM_{2.5}$ increased, with concentrations of 109.3 ± 16.0 $\mu g/m^3$. $PM_{2.5}$ continued to increase to an average of 159.4 $\mu g/m^3$ between the 22nd and 26th of January during which two significant $PM_{2.5}$ accumulation events were observed. The first accumulation (Event I, Figure 2A) started on January 23, 13:30 and lasted for 33 h, during which the $PM_{2.5}$ concentration more than doubled, from 104.0 to 268.3 $\mu g/m^3$. This was followed by a 2 h light precipitation (~1 mm), which rinsed out some of the $PM_{2.5}$, decreasing its concentration to 134.0 $\mu g/m^3$ within 15 h. A subsequent $PM_{2.5}$ accumulation period (Event II) occurred within 24 h, when the $PM_{2.5}$ concentration increased from 134.0 to 243.7 $\mu g/m^3$. Sulfate aerosol concentrations followed trends similar to $PM_{2.5}$ concentrations and mirrored the two rapid accumulation events. During Event I, sulfates have increased from 21.0 to 58.5 $\mu g/m^3$ in 27 h (an accumulation rate of 1.39 $\mu g/m^3/h$), and during Event II, sulfates have increased from 24.4 to 71.8 $\mu g/m^3$ within 21 h (an accumulation rate of 2.26 $\mu g/m^3/h$). Primary sulfate (includes the soil sulfate, the sea-salt sulfate, and the sulfate directly emitted with SO_2) was determined to be trivial during these events. Low concentrations of Ca^{2+} (1.88 ± 1.09 $\mu g/m^3$) and Na^+ (0.97 ± 0.86 $\mu g/m^3$) in the aerosols indicated that contribution of sulfates from soil entrainment[53] (SO_4^{2-}/Ca^{2+} = 0.18) and sea-salt aerosols[54] (SO_4^{2-}/Na^+ = 0.25) should be less than 0.58 $\mu g/m^3$, corresponding to <2% of the total sulfate observed. The primary sulfate emitted with SO_2 during coal burning has been estimated to be only <4% of SO_2 emission,[10,55] which based on observed SO_2 concentrations, would average at 1.66 ± 0.6 $\mu g/m^3$ during the sampling period (Figure 2A). Thus, the total primary sulfate only contributed for <6% of the total sulfate, indicating that most were the secondary sulfate (i.e., SO_2 oxidation). Additionally, the wind speed during the entire haze episode averaged at 1.03 ± 0.71 m/s with a maximum 3 h wind speed of 2.58 m/s (wind rose in Figure 1), indicating air stagnation. Considering the short lifetime[31] of atmospheric SO_2 (~12 h) and aerosols (~5 days) and the relatively low sulfur emissions outside of Nanjing within 200 km inferred from SO_2 emission inventory,[56] long-range transportation of $SO_{2(g)}$ and sulfates should be minor; thus, local SO_2 emissions and oxidation within Nanjing should be the dominant source of aerosol sulfate.

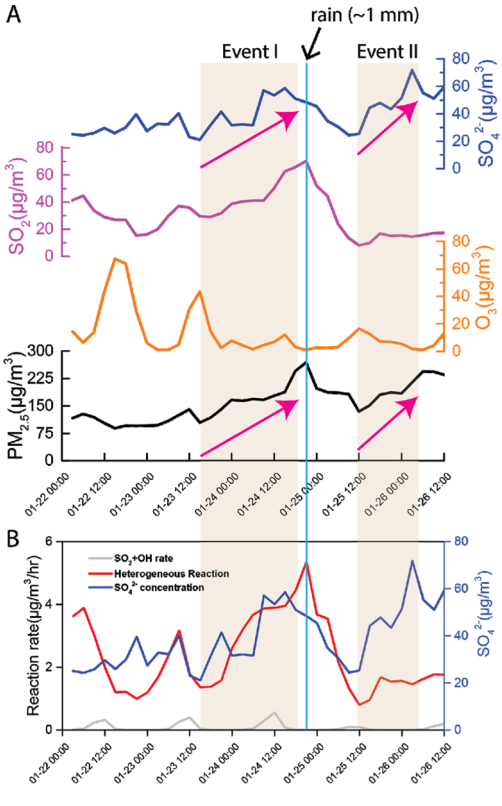

Figure 2. (A) Concentrations of sulfates, SO_2, O_3, and $PM_{2.5}$ during the haze episode. Shaded areas indicated two rapid $PM_{2.5}$ and sulfate accumulation events, and the blue line indicated a small rain event during the sampling period; (B) calculated reaction rates of SO_2 + OH (gray) and heterogeneous reaction (red) plotted with sulfate concentrations (blue).

The measured $\delta^{34}S_{sulfate}$ values were significantly higher than the estimated $\delta^{34}S_{emission}$ values in Nanjing,[38,39,44] showing a ~5‰ variation throughout the sampling period and displayed a negative correlation with the SO_2 oxidation ratio (SOR = $SO_4^{2-}/(SO_4^{2-} + SO_2)$). $\delta^{34}S_{sulfate}$ values (Figure 3A) in our samples ranged from +4.3 to +9.4‰ with an average of 6.2‰, similar to the values observed in a number of other Chinese megacities.[23,44−46] Because of air stagnation, SO_2 likely originated from local emissions, the majority of which in Nanjing was coal combustion with a $\delta^{34}S$ value of 3.0 ± 0.9‰.[43] Several studies have measured the $\delta^{34}S$ values of both SO_2 and sulfates simultaneously at Nanjing, showing that the $\delta^{34}S_{emission}$ ($\delta^{34}S_{emission} = \delta^{34}S_{SO_2} \times (1 - SOR) + \delta^{34}S_{SO_4^{2-}} \times SOR$) was +4.0 ± 0.1‰[44] in 1997 and 2.4 ± 0.6‰[38] in fall 2014. Chen et al.[39] have analyzed the $\delta^{34}S_{emission}$ in Nanjing prior to our sampling period (daily SO_2 and sulfate samples from January 1 to 23, while this work sampled 3 h sulfate samples from January 22 to 26) and found a constant $\delta^{34}S_{emission}$ value of 2.7 ± 1.0‰.[39] Therefore, we suggest that the $\delta^{34}S_{emission}$ value during our sampling period should also be 2.7 ± 1.0‰ (Figure 3A). These values are in good agreement with the SO_2 emission inventory,[56] which suggested that over 96% SO_2 emission in winter in the Nanjing area was from industrial and coal-burning power plants, which had a $\delta^{34}S$ value of 3 ± 3‰.[44,57] The measured $\delta^{34}S_{sulfate}$ values were significantly higher than the $\delta^{34}S_{emission}$, suggesting enrichment of ^{34}S in the sulfate and hence a depletion of ^{34}S in the remaining SO_2. This phenomenon has been observed in other studies, where the $\delta^{34}S$ values of the aerosol sulfate were usually 0−8‰ higher than the coexisting SO_2[38,39,41,44,58,59] but

https://dx.doi.org/10.1021/acs.est.9b07150
Environ. Sci. Technol. 2020, 54, 2626−2634

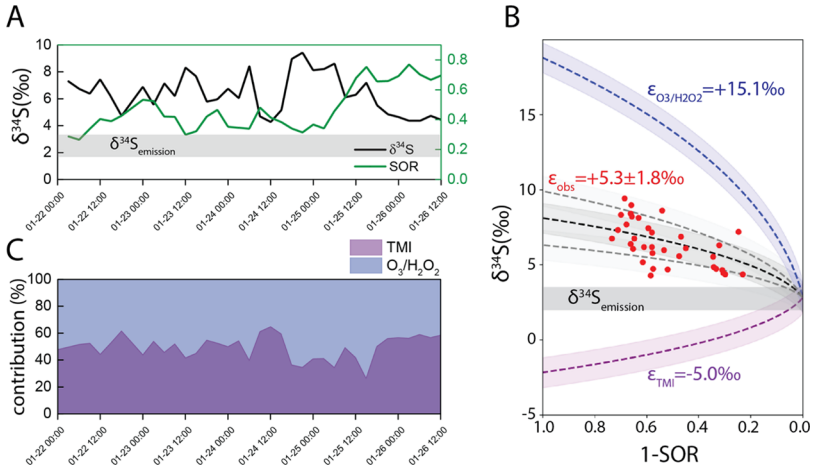

Figure 3. (A) Measured $\delta^{34}S_{sulfate}$ (black) and the calculated sulfur oxidation ratio (SOR, green) throughout the sampling period and compared with the estimated $\delta^{34}S_{emission}$ (gray bar); (B) Rayleigh distillation model of sulfate production. The gray bar indicates the $\delta^{34}S_{emission}$ (+2.7 ± 1.0‰) in Nanjing, red circles are the measured $\delta^{34}S_{sulfate}$ value in this study. Dashed lines with shaded areas are calculated $\delta^{34}S_{sulfate}$ values based on the $\delta^{34}S_{emission}$, the blue line indicates the $\delta^{34}S_{sulfate}$ value when SO_2 is oxidized solely by O_3 and H_2O_2, the purple line indicates the $\delta^{34}S_{sulfate}$ value when SO_2 is oxidized solely by TMI oxidation, the black line is the estimated ε value of +5.3‰, and two gray lines represent the upper and lower limits for the estimated ε values (+3.5 and +7.1‰). (C) Relative contributions of TMI and O3/H2O2 oxidations during the sampling period.

this phenomenon was not quantitatively explained. Also, the $\delta^{34}S_{sulfate}$ values showed a ~5.1‰ variation throughout the sampling period. If the $\delta^{34}S_{emission}$ remains constant during our sampling period, this variation could be explained as a result of sulfur isotopic fractionation during the oxidation process. Furthermore, we observed a negative correlation (slope = −6.2 and r = 0.6, Figure 3A,B) between SOR and the $\delta^{34}S$ value of sulfates in our samples, indicating that as oxidation of SO_2 progressed, the $\delta^{34}S$ values of sulfates decreased, making them approach $\delta^{34}S_{emission}$ (by isotope mass balance). This negative correlation supported our hypothesis that the elevated and variable $\delta^{34}S_{sulfate}$ values should be attributed to the isotopic fractionation during SO_2 oxidation processes.

The discrepancies between $\delta^{34}S_{sulfate}$ and $\delta^{34}S_{emission}$ (therefore, $\delta^{34}S_{SO_2}$) values have been observed, especially at low SOR levels. Forrest and Newman[59] measured $\delta^{34}S$ values of $SO_{2(g)}$ and sulfate particles in a polluted environment with a very low SOR (average SOR = 9.9% among the three experiments), and the $\delta^{34}S_{sulfate}$ values were ~1.5−2.5‰ higher than the $\delta^{34}SS_{SO_2}$ values. Saltzman[41] conducted a similar experiment at Hubbard Brook Experimental Forest, New Hampshire, and observed a ~3‰ difference between $\delta^{34}S_{sulfate}$ and $\delta^{34}S_{SO_2}$ values when the SOR was <40%. Later studies by Guo et al.[38] and Chen et al.[39] have suggested that the $\delta^{34}S_{sulfate}$−$\delta^{34}S_{SO2}$ values at Nanjing ranged between ~1 and 7‰ during fall 2014 and winter 2015. These differences have suggested that the $\delta^{34}S_{sulfate}$ values may deviate from the $\delta^{34}S_{emission}$ values by several permil, especially when the SOR value was low. This deviation might complicate the use of $\delta^{34}S_{sulfate}$ to calculate the sources of SO_2 in urban regions, since most urban (anthropogenic) SO_2 sources have a narrow range of $\delta^{34}S$ values[45,57] (+1 to +11‰), which could be potentially altered by the isotopic fractionations during the formation of the sulfate when the SOR was low. This uncertainty might be reduced by analyzing other minor sulfur isotopes (^{33}S, ^{35}S, and ^{36}S)[47−51] but this is beyond the scope of our work. Therefore, extra caution must be taken when using $\delta^{34}S$ values to estimate the sources of SO_2 in the urban environment with the low SOR.

The observed differences in $\delta^{34}S_{sulfate}$ and $\delta^{34}S_{emission}$ values can be explained using the Rayleigh distillation model, and the isotopic enrichment factor ($\varepsilon = (\alpha - 1) \times 1000‰$) for the total oxidation processes can also be quantified. The Rayleigh distillation model[42,60] is used to calculate the kinetic isotopic fractionation of a reaction (A → B) in an open system by assuming no isotopic exchange between A and B. In aqueous solution, $SO_{2(g)}$ dissolving into aerosol water was 2−3 orders of magnitude faster than the subsequent oxidation into SO_4^{2-}; thus, the isotopic fractionation should be controlled by the kinetic isotopic effect occurring during any aqueous SO_2 oxidation process.[35] In this model, the $\delta^{34}S$ value of SO_2 is a function of $\delta^{34}S_{emission}$, the fraction (f) of remaining SO_2 (f = 1 − SOR), and the observed fractionation factor of the oxidation process (ε_{obs})

$$\delta^{34}S_{SO_2} = \delta^{34}S_{emission} + \ln(f) \times \varepsilon_{obs} \quad (1)$$

Thus $\delta^{34}S_{sulfate}$ is

$$\delta^{34}S_{sulfate} = \delta^{34}S_{emission} - \varepsilon_{obs} \times \ln(f) \times f/(1-f) \quad (2)$$

Using the observed $\delta^{34}S_{sulfate}$, f, and the estimated $\delta^{34}S_{emission}$ during our sampling period (2.7 ± 1.0‰), we found that the ε_{obs} values ranged from 2.2 to 10.0‰ (Figure 3B) with an average value of +5.3 ± 1.8‰ (1σ).

This changing ε_{obs} value suggests that multiple SO_2 oxidation pathways have contributed to the observed sulfate accumulation. At 273 K (average temperature during the sampling period), OH oxidation enriches ^{34}S in the product sulfate with an enrichment factor (ε_{OH}) of +11.0‰,[35] and oxidation by the TMI pathway depletes ^{34}S (ε_{TMI} = −5.0‰) in the product sulfate with a ε_{TMI} value of −5.0‰.[35,36] Several laboratory experiments[35−37] measured the ε values of SO_2 + O_3 and SO_2 + H_2O_2, and these two pathways showed similar ε values ranging from +15.1 to +17.4‰. Therefore, here we use ε_{O_3/H_2O_2} = +15.1‰ to represent the combined isotopic effect of O_3 and/or H_2O_2 pathways. Since the variation of temperature during the entire sampling period was small (the standard deviation of ±3.7 K), the variations of the fractionation factors (<1‰) were insignificant comparing to the differences

https://dx.doi.org/10.1021/acs.est.9b07150
Environ. Sci. Technol. 2020, 54, 2626−2634

between the fractionation factors (~20‰). Therefore, in the following calculation, we assume that the fractionation factors are constants. The ε_{obs} value does not agree with any of the laboratory-determined ε values, suggesting that none of the pathways had a dominant role in the formation of the sulfate. Instead, the ε_{obs} should be a result of the mixing of multiple oxidation pathways

$$\varepsilon_{obs} = \varepsilon_{O_3/H_2O_2} \times f_{O_3/H_2O_2} + \varepsilon_{TMI} \times f_{TMI} + \varepsilon_{OH} \times f_{OH} \quad (3)$$

in which ε_i and f_i are the enrichment factor and the contribution of the pathway i, and $f_{O_3/H_2O_2} + f_{TMI} + f_{OH} = 1$.

The sulfate formed via the gas-phase SO_2 + OH pathway was calculated to be unimportant. Concentrations of the OH radical were first obtained using a zero-dimensional (0-D) atmospheric chemistry model coupled with time-dependent photochemistry. The model used the tropospheric ultraviolet and visible (TUV) radiation model[61] to determine the molecular photolysis frequencies (j values) for the major molecules (O_3, NO_2, NO_3, HONO, N_2O_5, H_2O_2, and other organic molecules) during the sampling period for a time step of 3 h. Subsequently calculated j values were incorporated into a 0-D atmospheric chemistry model driven by the "regional atmospheric chemistry modeling" (RACM) mechanism.[62] The model then calculated time-dependent OH radical concentrations using average concentrations of trace gases (O_3, H_2O, NO_2, SO_2, CO, and CH_4) during the pollution period. The OH concentrations display clear diurnal variation, with the peak concentration of 1.35×10^6 molecules/cm^3 at noon, and a daily average value of 0.31×10^6 molecules/cm^3, similar to the observed winter OH concentrations in other urban areas.[63,64] The reaction rates of gas-phase SO_2 oxidation (SO_2 + OH) were then calculated using

$$d[SO_4^{2-}]/dt = k \times [SO_2] \times [OH] \quad (4)$$

in which k is the reaction constant[5] at 273 K (1.5×10^{-12} molecules^{-1} × cm^3 × s^{-1}), [SO_2] and [OH] are observed SO_2 concentrations and calculated OH concentrations. The results (the gray line in Figure 2B) suggest that the OH oxidation rate averaged at 0.05 μg/m^3/h during the entire sampling period, and the maximum oxidation rate with the highest OH concentration at noon was only 0.3 μg/m^3/h. Since the measured sulfate accumulation rates were 1.3 and 2.1 μg/m^3/h during the two accumulation events, and assuming a negligible sulfate dry deposition of 0.1 cm/s[65] and an average boundary layer height of 600 m, the sulfate production rates during the two events were 1.55 and 2.38 μg/m^3/h. These estimated sulfate production rates were 26−46 times faster than the average OH oxidation rate. A similar low sulfate production via gas-phase oxidation was also inferred during winter haze episodes in Beijing.[17] This low contribution (2−3%) of gas-phase sulfate production was probably because of a combination of weak photochemistry in winter, a high aerosol concentration that scattered light, and extremely high heterogeneous and aqueous oxidations in haze episodes.[11,66,67] Therefore, O_3, H_2O_2, and TMI pathways should be the dominant contributors to the observed high sulfate production, and eq 3 can be simplified as

$$\varepsilon_{obs} = \varepsilon_{O_3/H_2O_2} \times f_{O_3/H_2O_2} + \varepsilon_{TMI} \times f_{TMI} \quad (5)$$

Equation 5 can be used to estimate the role of heterogeneous and aqueous oxidations of $SO_{2(g)}$ by O_3, H_2O_2, and TMI-catalyzed O_2 that were likely to be responsible for the fast accumulation of sulfate aerosols during the haze episode. This hypothesis is further confirmed by applying a pseudo-first-order uptake process to estimate heterogeneous and aqueous sulfate production.[1] This approach treats SO_2 oxidation on/in the aerosols as a first-order uptake reaction on the surface of the aerosols:

$$SO_{2(g)} + \text{aerosol} \rightarrow \text{sulfate}$$

Its rate is expressed as[1,17,68]

$$d[SO_4^{2-}]/dt_{het} = (R_a/D_g + 4/\gamma\nu)^{-1} \times S_a \times [SO_2] \quad (6)$$

in which D_g (2×10^{-5}) is the SO_2 diffusion coefficient,[68] ν (300 m^2/s) is the SO_2 mean molecular velocity,[68] and R_a is the effective radius of aerosols, which is estimated using the following equation that was empirically derived from two haze episodes in Beijing[2]

$$R_a = (0.254 \times [PM_{2.5}]/(\mu g/m^3) + 10.259) \times 10^{-9}\ m \quad (7)$$

S_a is the aerosol surface area density (cm^2/cm^3) estimated using the average aerosol effective radius and the average density (ρ) of $PM_{2.5}$ (1.5 g/cm^3)

$$S_a = [PM_{2.5}] \times 3/(R_a \times \rho) \quad (8)$$

and γ is the SO_2 uptake coefficient. Although laboratory-determined γ values of SO_2 uptake can vary by several orders of magnitude depending on the surface property, particle compositions, temperature, and RH, previous modeling works have shown that setting the average γ values as a function of relative humidity[1] would best match the modeled sulfate to observations

$$\gamma = \max(2.0 \times 10^{-5},\ 6.0 \times 10^{-7} \times RH(\%) - 1 \times 10^{-5}) \quad (9)$$

The calculated sulfate production rates ranged from 0.8 to 5.2 μg/m^3/h with a mean value of 2.3 μg/m^3/h during the sampling period (Figure 2B), similar to the observed sulfate accumulation rates (1.5 and 2.1 μg/m^3/h). Therefore, this calculation implies that heterogeneous and aqueous oxidations via O_3, H_2O_2, and TMI pathways were the main sources of sulfates during the haze episode. The overall calculated sulfate production rate agrees well with the observed data, but this approach seems to be overestimating the sulfate production during Event I by ~80% (2.79 μg/m^3/h vs observed 1.55 μg/m^3/h) and underestimating the sulfate production in Event II by ~44% (1.32 μg/m^3/h vs observed 2.38 μg/m^3/h). Since the $PM_{2.5}$ mass and hence aerosol surface area were similar between the two events (141 ± 41 μg/m^3 in Event I vs 171 ± 24 μg/m^3 in Event II) but the RH in Event II (81 ± 2%) was higher than Event I (57 ± 17%), and that the SO_2 uptake coefficient is a function of RH, we suggest that this discrepancy might be due to the over-/underestimation of the SO_2 uptake coefficient at low/high RH. The calculated SO_2 uptake coefficient ranged from 2×10^{-5} to 5×10^{-5} but experimental data has shown that these coefficients are a function of the aerosol surface material. SO_2 uptake coefficients can be as low[69] as 0.41×10^{-5} on Sahara dust or as high[70] as 6.6×10^{-5} on iron oxides. Therefore, we suggest that the pseudo-first-order uptake process estimation[1] showed general agreement with the observed average production rate, although it is

https://dx.doi.org/10.1021/acs.est.9b07150
Environ. Sci. Technol. 2020, 54, 2626−2634

possible to under-/overestimate the uptake coefficients (therefore the oxidation rate) over a short time period at certain conditions because of the heterogeneity of aerosol compositions.

These calculations suggest that the sulfate in the haze episode was primarily controlled by the heterogeneous and aqueous oxidations via O_3, H_2O_2, and TMI pathways, enabling us to use the ε_{obs} and eq 5 to estimate the contributions of the oxidation pathways. The overall ε_{obs} value (+5.3 ± 1.8‰) falls in between ε_{O_3/H_2O_2} and ε_{TMI} values, indicating that both O_3/H_2O_2 and TMI pathways played important roles in the oxidation process. Using eq 5, we determined that the overall contributions from TMI and O_3/H_2O_2 pathways (Figure 3C) were roughly equal (f_{TMI} = 49 ± 10% and f_{O_3/H_2O_2} = 51 ± 10%) during the haze episode. Notably, however, there were two time periods (at the end of $PM_{2.5}$ accumulation events I and II) when decreases in the ε_{obs} values were observed. In the first time period (January 24, 6:00−18:00), the sulfate concentration increased by ∼100%, the SOR remained steady, while the $\delta^{34}S_{sulfate}$ values decreased from 8.4 to +4.6‰. The calculated ε_{obs} values, thus, have decreased from 7.2 to 2.8‰, suggesting that the TMI pathway has played a more important role during this process. The second time period (January 25, 12:00 to January 26, 3:00) was similar when the sulfate concentration increased by ∼180% and the ε_{obs} value decreased from 9.9 to 3.4‰. Both events were associated with high $PM_{2.5}$ and low O_3 concentrations. The decreased ε_{obs} values suggested elevated contributions of the TMI pathway (accounting for 57−62% of sulfate production). The increased TMI pathway contribution likely resulted from a combination of two factors. First, the high aerosol concentrations, which likely provided a high aerosol surface area and a high amount of transition-metal ions (e.g., Fe, Mn, Cu, Zn, and Pb), from local industrial emission[71] could enhance the rate of TMI oxidation. Second, the O_3/H_2O_2 oxidation rate was likely decreased due to decreased O_3 concentrations and the liquid water content. The average O_3 concentrations (6.2 and 5.0 $\mu g/m^3$) and RH (51 and 65%) during these two periods were significantly lower than those of the rest of the haze episode (averaging 13.0 $\mu g/m^3$ O_3 and 81% RH), which might reduce the oxidation rate of O_3/H_2O_2. However, since it is difficult to quantitatively determine the rate of the TMI pathway and the accurate pH of aerosol water, therefore, the rate of O_3 oxidation, either the factor or both factors could be the dominant cause. A future experimental work is needed to separately investigate the effects of the aerosol surface area, transition-metal ion concentrations, RH, O_3 concentration, etc., on each oxidation pathway.

The significant contribution from the TMI pathway (49 ± 10%) suggests an elevated role of the TMI pathway during the rapid formation of sulfate aerosols in the haze episode, showing general agreement with atmospheric chemistry modeling studies. Globally, the TMI pathway was estimated to contribute to 9−18% of total aerosol production,[8,10] in most regions in China (including Nanjing); model simulations suggested that TMI had played a more important role, contributing to ∼20−50% of total sulfate production.[10] Harris et al.[35] also pointed out that at least 35% of the sulfate in several Chinese cities[44] was produced via the TMI pathway. During haze episodes, the contributions of the TMI pathway among the heterogeneous and aqueous oxidations seem to increase; a recently developed modeling study[22] suggests that the TMI pathway was responsible for as much as 80% of total heterogeneous and aqueous sulfate production during haze episodes in Beijing, and oxygen isotopic evidence suggested similar contributions (66−73%).[17] Furthermore, the field observation work at another heavily polluted region (Fort McMurray, Alberta, Canada) also implied the importance of the TMI pathway during the formation of the secondary sulfate.[72] Our study had pointed out that the TMI pathway was an important but probably not the sole sulfate formation pathway during the haze episodes, and its contribution was likely elevated during the haze episodes. The increased contribution of the TMI pathway during haze episodes might originate from a combination of high aerosol surface, high atmospheric liquid water content, and dust flux. In the meantime, the O_3 and/or H_2O_2 also played a major role in the formation of sulfate aerosols despite their lower-than-typical concentrations. Therefore, to improve the simulation of sulfate aerosol formation, all of the above reactions (aqueous O_3, H_2O_2, and TMI oxidations and heterogeneous O_3, H_2O_2, and TMI oxidations) should be carefully parameterized in atmospheric chemistry models.

AUTHOR INFORMATION

Corresponding Author

Yan-Lin Zhang − *Yale−NUIST Center on Atmospheric Environment, Joint International Research Laboratory of Climate and Environment Change (ILCEC), Key Laboratory of Meteorological Disaster Ministry of Education (KLME), Collaborative Innovation Center on Forecast and Evaluation of Meteorological Disasters (CIC-FEMD), and School of Applied Meteorology, Nanjing University of Information Science and Technology, Nanjing 210044, China;* orcid.org/0000-0002-8722-8635; Email: dryanlinzhang@outlook.com, zhangyanlin@nuist.edu.cn

Authors

Jianghanyang Li − *Department of Earth, Atmospheric and Planetary Sciences, Purdue University, West Lafayette, Indiana 47907, United States;* orcid.org/0000-0003-4965-0031

Fang Cao − *Yale−NUIST Center on Atmospheric Environment, Joint International Research Laboratory of Climate and Environment Change (ILCEC), Key Laboratory of Meteorological Disaster Ministry of Education (KLME), Collaborative Innovation Center on Forecast and Evaluation of Meteorological Disasters (CIC-FEMD), and School of Applied Meteorology, Nanjing University of Information Science and Technology, Nanjing 210044, China*

Wenqi Zhang − *Yale−NUIST Center on Atmospheric Environment, Joint International Research Laboratory of Climate and Environment Change (ILCEC), Key Laboratory of Meteorological Disaster Ministry of Education (KLME), Collaborative Innovation Center on Forecast and Evaluation of Meteorological Disasters (CIC-FEMD), and School of Applied Meteorology, Nanjing University of Information Science and Technology, Nanjing 210044, China*

Meiyi Fan − *Yale−NUIST Center on Atmospheric Environment, Joint International Research Laboratory of Climate and Environment Change (ILCEC), Key Laboratory of Meteorological Disaster Ministry of Education (KLME), Collaborative Innovation Center on Forecast and Evaluation of Meteorological Disasters (CIC-FEMD), and School of Applied Meteorology, Nanjing University of Information Science and Technology, Nanjing 210044, China*

https://dx.doi.org/10.1021/acs.est.9b07150
Environ. Sci. Technol. 2020, 54, 2626−2634

Xuhui Lee − *School of Forestry and Environmental Studies, Yale University, New Haven, Connecticut 06520, United States; Yale−NUIST Center on Atmospheric Environment, Joint International Research Laboratory of Climate and Environment Change (ILCEC), Nanjing University of Information Science and Technology, Nanjing 210044, China*

Greg Michalski − *Department of Earth, Atmospheric and Planetary Sciences and Department of Chemistry, Purdue University, West Lafayette, Indiana 47907, United States*

Complete contact information is available at: https://pubs.acs.org/10.1021/acs.est.9b07150

Notes

The authors declare no competing financial interest.

■ ACKNOWLEDGMENTS

The authors thank funding support from the National Nature Science Foundation of China (No. 41977305), National Key R&D Program of China (Nos. 2017YFC0212704 and 2017YFC0210101), the Provincial Natural Science Foundation of Jiangsu (No. BK20180040), Jiangsu Innovation & Entrepreneurship Team, the National Science Foundation of U.S., Purdue Climate Change Research Center, and the Advanced Study Program from National Center for Atmospheric Research, U.S.

■ REFERENCES

(1) Zheng, B.; Zhang, Q.; Zhang, Y.; He, K. B.; Wang, K.; Zheng, G. J.; Duan, F. K.; Ma, Y. L.; Kimoto, T. Heterogeneous Chemistry: A Mechanism Missing in Current Models to Explain Secondary Inorganic Aerosol Formation during the January 2013 Haze Episode in North China. *Atmos. Chem. Phys.* **2015**, *15*, 2031−2049.

(2) Guo, S.; Hu, M.; Zamora, M. L.; Peng, J.; Shang, D.; Zheng, J.; Du, Z.; Wu, Z.; Shao, M.; Zeng, L.; et al. Elucidating Severe Urban Haze Formation in China. *Proc. Natl. Acad. Sci. U.S.A.* **2014**, *111*, 17373−17378.

(3) Zheng, G. J.; Duan, F. K.; Su, H.; Ma, Y. L.; Cheng, Y.; Zheng, B.; Zhang, Q.; Huang, T.; Kimoto, T.; Chang, D.; et al. Exploring the Severe Winter Haze in Beijing: The Impact of Synoptic Weather, Regional Transport and Heterogeneous Reactions. *Atmos. Chem. Phys.* **2015**, *15*, 2969−2983.

(4) Huang, R.-J.; Zhang, Y.; Bozzetti, C.; Ho, K.-F.; Cao, J.-J.; Han, Y.; Daellenbach, K. R.; Slowik, J. G.; Platt, S. M.; Canonaco, F.; et al. High Secondary Aerosol Contribution to Particulate Pollution during Haze Events in China. *Nature* **2014**, *514*, 218.

(5) Atkinson, R.; Baulch, D. L.; Cox, R. A.; Crowley, J. N.; Hampson, R. F.; Hynes, R. G.; Jenkin, M. E.; Rossi, M. J.; Troe, J. Evaluated Kinetic and Photochemical Data for Atmospheric Chemistry: Volume I-Gas Phase Reactions of O_x, HO_x, NO_x and SO_x Species. *Atmos. Chem. Phys.* **2004**, *4*, 1461−1738.

(6) Reid, J. S.; Jonsson, H. H.; Smith, M. H.; Smirnov, A. Evolution of the Vertical Profile and Flux of Large Sea-salt Particles in a Coastal Zone. *J. Geophys. Res.: Atmos.* **2001**, *106*, 12039−12053.

(7) Herrmann, H.; Ervens, B.; Jacobi, H.-W.; Wolke, R.; Nowacki, P.; Zellner, R. CAPRAM2. 3: A Chemical Aqueous Phase Radical Mechanism for Tropospheric Chemistry. *J. Atmos. Chem.* **2000**, *36*, 231−284.

(8) Sofen, E. D.; Alexander, B.; Kunasek, S. A. The Impact of Anthropogenic Emissions on Atmospheric Sulfate Production Pathways, Oxidants, and Ice Core $\Delta^{17}O$ (SO_4^{2-}). *Atmos. Chem. Phys.* **2011**, *11*, 3565−3578.

(9) Harris, E.; Sinha, B.; van Pinxteren, D.; Tilgner, A.; Fomba, K. W.; Schneider, J.; Roth, A.; Gnauk, T.; Fahlbusch, B.; Mertes, S.; Lee, T.; Collett, J.; Foley, S.; Borrmann, S.; Hoppe, P.; Herrmann, H. Enhanced Role of Transition Metal Ion Catalysis during In-Cloud Oxidation of SO_2. *Science* **2013**, *340*, 727−730.

(10) Alexander, B.; Park, R. J.; Jacob, D. J.; Gong, S. Transition Metal-Catalyzed Oxidation of Atmospheric Sulfur: Global Implications for the Sulfur Budget. *J. Geophys. Res.* **2009**, *114*, No. D02309.

(11) Wang, G.; Zhang, R.; Gomez, M.; Yang, L.; Zamora, M. L.; Hu, M.; Lin, Y.; Peng, J.; Guo, S.; Meng, J.; Li, J.; Cheng, C.; Hu, T.; Ren, Y.; Wang, Y.; Gao, J.; Cao, J.; An, Z.; Zhou, W.; Li, G.; Wang, J.; Tian, P.; Marrero-Ortiz, W.; Secrest, J.; Du, Z.; Zheng, J.; Shang, D.; Zeng, L.; Shao, M.; Wang, W.; Huang, Y.; Wang, Y.; Zhu, Y.; Li, Y.; Hu, J.; Pan, B.; Cai, L.; Cheng, Y.; Ji, Y.; Zhang, F.; Rosenfeld, D.; Liss, P.; Duce, R.; Kolb, C.; Molina, M. Persistent Sulfate Formation from London Fog to Chinese Haze. *Proc. Natl. Acad. Sci. U.S.A.* **2016**, *113*, 13630−13635.

(12) Cheng, Y.; Zheng, G.; Wei, C.; Mu, Q.; Zheng, B.; Wang, Z.; Gao, M.; Zhang, Q.; He, K.; Carmichael, G.; et al. Reactive Nitrogen Chemistry in Aerosol Water as a Source of Sulfate during Haze Events in China. *Sci. Adv.* **2016**, *2*, No. e1601530.

(13) Xue, J.; Yuan, Z.; Yu, J. Z.; Lau, A. K. H. An Observation-Based Model for Secondary Inorganic Aerosols. *Aerosol Air Qual. Res.* **2014**, *14*, 862−878.

(14) Xue, J.; Yuan, Z.; Griffith, S. M.; Yu, X.; Lau, A. K. H.; Yu, J. Z. Sulfate Formation Enhanced by a Cocktail of High NO_x, SO_2, Particulate Matter, and Droplet PH during Haze-Fog Events in Megacities in China: An Observation-Based Modeling Investigation. *Environ. Sci. Technol.* **2016**, *50*, 7325−7334.

(15) Li, G.; Bei, N.; Cao, J.; Huang, R.; Wu, J.; Feng, T.; Wang, Y.; Liu, S.; Zhang, Q.; Tie, X.; Molina, L. T. A Possible Pathway for Rapid Growth of Sulfate during Haze Days in China. *Atmos. Chem. Phys.* **2017**, *17*, 3301−3316.

(16) Huang, X.; Song, Y.; Zhao, C.; Li, M.; Zhu, T.; Zhang, Q.; Zhang, X. Pathways of Sulfate Enhancement by Natural and Anthropogenic Mineral Aerosols in China. *J. Geophys. Res.: Atmos.* **2014**, *119*, 14,165−14,179.

(17) He, P.; Alexander, B.; Geng, L.; Chi, X.; Fan, S.; Zhan, H.; Kang, H.; Zheng, G.; Cheng, Y.; Su, H.; Liu, C.; Xie, Z. Isotopic Constraints on Heterogeneous Sulfate Production in Beijing Haze. *Atmos. Chem. Phys.* **2018**, *18*, 5515−5528.

(18) Li, L.; Hoffmann, M. R.; Colussi, A. J. Role of Nitrogen Dioxide in the Production of Sulfate during Chinese Haze-Aerosol Episodes. *Environ. Sci. Technol.* **2018**, *52*, 2686−2693.

(19) Liu, C.; Ma, Q.; Liu, Y.; Ma, J.; He, H. Synergistic Reaction between SO_2 and NO_2 on Mineral Oxides: A Potential Formation Pathway of Sulfate Aerosol. *Phys. Chem. Chem. Phys.* **2012**, *14*, 1668−1676.

(20) Zhao, D.; Song, X.; Zhu, T.; Zhang, Z.; Liu, Y.; Shang, J. Multiphase Oxidation of SO_2 by NO_2 on $CaCO_3$ Particles. *Atmos. Chem. Phys.* **2018**, *18*, 2481−2493.

(21) Wang, G.; Huang, L.; Gao, S.; Gao, S.; Wang, L. Characterization of Water-Soluble Species of PM_{10} and $PM_{2.5}$ Aerosols in Urban Area in Nanjing, China. *Atmos. Environ.* **2002**, *36*, 1299−1307.

(22) Shao, J.; Chen, Q.; Wang, Y.; Lu, X.; He, P.; Sun, Y.; Shah, V.; Martin, R. V.; Philip, S.; Song, S.; et al. Heterogeneous Sulfate Aerosol Formation Mechanisms during Wintertime Chinese Haze Events: Air Quality Model Assessment Using Observations of Sulfate Oxygen Isotopes in Beijing. *Atmos. Chem. Phys.* **2019**, *19*, 6107−6123.

(23) Li, X.; Bao, H.; Gan, Y.; Zhou, A.; Liu, Y. Multiple Oxygen and Sulfur Isotope Compositions of Secondary Atmospheric Sulfate in a Mega-City in Central China. *Atmos. Environ.* **2013**, *81*, 591−599.

(24) Zhang, R.; Wang, G.; Guo, S.; Zamora, M. L.; Ying, Q.; Lin, Y.; Wang, W.; Hu, M.; Wang, Y. Formation of Urban Fine Particulate Matter. *Chem. Rev.* **2015**, *115*, 3803−3855.

(25) Wang, J.; Wang, S.; Jiang, J.; Ding, A.; Zheng, M.; Zhao, B.; Wong, D. C.; Zhou, W.; Zheng, G.; Wang, L.; et al. Impact of Aerosol−Meteorology Interactions on Fine Particle Pollution during China's Severe Haze Episode in January 2013. *Environ. Res. Lett.* **2014**, *9*, No. 094002.

(26) Wang, Y.; Zhang, Q.; Jiang, J.; Zhou, W.; Wang, B.; He, K.; Duan, F.; Zhang, Q.; Philip, S.; Xie, Y. Enhanced Sulfate Formation during China's Severe Winter Haze Episode in January 2013 Missing

from Current Models. *J. Geophys. Res.: Atmos.* **2014**, *119*, 10,425−10,440.
(27) Liu, M.; Song, Y.; Zhou, T.; Xu, Z.; Yan, C.; Zheng, M.; Wu, Z.; Hu, M.; Wu, Y.; Zhu, T. Fine Particle pH during Severe Haze Episodes in Northern China. *Geophys. Res. Lett.* **2017**, *44*, 5213−5221.
(28) Shi, G.; Xu, J.; Peng, X.; Xiao, Z.; Chen, K.; Tian, Y.; Guan, X.; Feng, Y.; Yu, H.; Nenes, A.; Russell, A. G. PH of Aerosols in a Polluted Atmosphere: Source Contributions to Highly Acidic Aerosol. *Environ. Sci. Technol.* **2017**, *51*, 4289−4296.
(29) Weber, R. J.; Guo, H.; Russell, A. G.; Nenes, A. High Aerosol Acidity despite Declining Atmospheric Sulfate Concentrations over the Past 15 Years. *Nat. Geosci.* **2016**, *9*, 282.
(30) Fountoukis, C.; Nenes, A. ISORROPIA II: A Computationally Efficient Thermodynamic Equilibrium Model for K^+−Ca^{2+}−Mg^{2+}−NH_4^+−Na^+−SO_4^{2-}−NO_3^-−Cl^-−H_2O Aerosols. *Atmos. Chem. Phys.* **2007**, *7*, 4639−4659.
(31) Seinfeld, J. H.; Pandis, S. N.; Noone, K. *Atmospheric Chemistry and Physics: From Air Pollution to Climate Change*; AIP, 1998; pp 265−324.
(32) Gankanda, A.; Coddens, E. M.; Zhang, Y.; Cwiertny, D. M.; Grassian, V. H. Sulfate Formation Catalyzed by Coal Fly Ash, Mineral Dust and Iron (III) Oxide: Variable Influence of Temperature and Light. *Environ. Sci.: Processes Impacts* **2016**, *18*, 1484−1491.
(33) Bao, H.; Thiemens, M. H.; Loope, D. B.; Yuan, X.-L. Sulfate Oxygen-17 Anomaly in an Oligocene Ash Bed in Mid-North America: Was It the Dry Fogs? *Geophys. Res. Lett.* **2003**, *30*, No. 1843.
(34) Bao, H.; Reheis, M. C. Multiple Oxygen and Sulfur Isotopic Analyses on Water-Soluble Sulfate in Bulk Atmospheric Deposition from the Southwestern United States. *J. Geophys. Res.* **2003**, *108*, No. 4430.
(35) Harris, E.; Sinha, B.; Hoppe, P.; Ono, S. High-Precision Measurements of ^{33}S and ^{34}S Fractionation during SO_2 Oxidation Reveal Causes of Seasonality in SO_2 and Sulfate Isotopic Composition. *Environ. Sci. Technol.* **2013**, *47*, 12174−12183.
(36) Harris, E.; Sinha, B.; Hoppe, P.; Foley, S.; Borrmann, S. Fractionation of Sulfur Isotopes during Heterogeneous Oxidation of SO_2 on Sea Salt Aerosol: A New Tool to Investigate Non-Sea Salt Sulfate Production in the Marine Boundary Layer. *Atmos. Chem. Phys.* **2012**, *12*, 4619−4631.
(37) Harris, E.; Sinha, B.; Hoppe, P.; Crowley, J. N.; Ono, S.; Foley, S. Sulfur Isotope Fractionation during Oxidation of Sulfur Dioxide: Gas-Phase Oxidation by OH Radicals and Aqueous Oxidation by H_2O_2, O_3 and Iron Catalysis. *Atmos. Chem. Phys.* **2012**, *12*, 407−424.
(38) Guo, Z.; Shi, L.; Chen, S.; Jiang, W.; Wei, Y.; Rui, M.; Zeng, G. Sulfur Isotopic Fractionation and Source Appointment of $PM_{2.5}$ in Nanjing Region around the Second Session of the Youth Olympic Games. *Atmos. Res.* **2016**, *174*−*175*, 9−17.
(39) Chen, S.; Guo, Z.; Guo, Z.; Guo, Q.; Zhang, Y.; Zhu, B.; Zhang, H. Sulfur Isotopic Fractionation and Its Implication: Sulfate Formation in $PM_{2.5}$ and Coal Combustion under Different Conditions. *Atmos. Res.* **2017**, *194*, 142−149.
(40) Li, J.; Michalski, G.; Davy, P.; Harvey, M.; Katzman, T.; Wilkins, B. Investigating Source Contributions of Size-Aggregated Aerosols Collected in Southern Ocean and Baring Head, New Zealand Using Sulfur Isotopes. *Geophys. Res. Lett.* **2018**, *45*, 3717−3727.
(41) Saltzman, E. S.; Brass, G. W.; Price, D. A. The Mechanism of Sulfate Aerosol Formation: Chemical and Sulfur Isotopic Evidence. *Geophys. Res. Lett.* **1983**, *10*, 513−516.
(42) Rayleigh, L. L. Theoretical Considerations Respecting the Separation of Gases by Diffusion and Similar Processes. *London, Edinburgh, Dublin Philos. Mag. J. Sci.* **1896**, *42*, 493−498.
(43) Maruyama, T.; Ohizumi, T.; Taneoka, Y.; Minami, N.; Fukuzaki, N.; Mukai, H.; Murano, K.; Kusakabe, M. Sulfur Isotope Ratios of Coals and Oils Used in China and Japan. *Nippon Kagaku Kaishi* **2000**, 45−52.
(44) Mukai, H.; Tanaka, A.; Fujii, T.; Zeng, Y.; Hong, Y.; Tang, J.; Guo, S.; Xue, H.; Sun, Z.; Zhou, J. Regional Characteristics of Sulfur and Lead Isotope Ratios in the Atmosphere at Several Chinese Urban Sites. *Environ. Sci. Technol.* **2001**, *35*, 1064−1071.
(45) Han, X.; Guo, Q.; Liu, C.; Fu, P.; Strauss, H.; Yang, J.; Hu, J.; Wei, L.; Ren, H.; Peters, M.; et al. Using Stable Isotopes to Trace Sources and Formation Processes of Sulfate Aerosols from Beijing, China. *Sci. Rep.* **2016**, *6*, No. 29958.
(46) Wei, L.; Yue, S.; Zhao, W.; Yang, W.; Zhang, Y.; Ren, L.; Han, X.; Guo, Q.; Sun, Y.; Wang, Z.; Fu, P. Stable Sulfur Isotope Ratios and Chemical Compositions of Fine Aerosols ($PM_{2.5}$) in Beijing, China. *Sci. Total Environ.* **2018**, *633*, 1156−1164.
(47) Guo, Z.; Li, Z.; Farquhar, J.; Kaufman, A. J.; Wu, N.; Li, C.; Dickerson, R. R.; Wang, P. Identification of Sources and Formation Processes of Atmospheric Sulfate by Sulfur Isotope and Scanning Electron Microscope Measurements. *J. Geophys. Res.* **2010**, *115*, No. D00K07.
(48) Han, X.; Guo, Q.; Strauss, H.; Liu, C.; Hu, J.; Guo, Z.; Wei, R.; Peters, M.; Tian, L.; Kong, J. Multiple Sulfur Isotope Constraints on Sources and Formation Processes of Sulfate in Beijing $PM_{2.5}$ Aerosol. *Environ. Sci. Technol.* **2017**, *51*, 7794−7803.
(49) Lin, M.; Biglari, S.; Zhang, Z.; Crocker, D.; Tao, J.; Su, B.; Liu, L.; Thiemens, M. H. Vertically Uniform Formation Pathways of Tropospheric Sulfate Aerosols in East China Detected from Triple Stable Oxygen and Radiogenic Sulfur Isotopes. *Geophys. Res. Lett.* **2017**, *44*, 5187−5196.
(50) Lin, M.; Zhang, X.; Li, M.; Xu, Y.; Zhang, Z.; Tao, J.; Su, B.; Liu, L.; Shen, Y.; Thiemens, M. H. Five-S-Isotope Evidence of Two Distinct Mass-Independent Sulfur Isotope Effects and Implications for the Modern and Archean Atmospheres. *Proc. Natl. Acad. Sci. U.S.A.* **2018**, *115*, 8541−8546.
(51) Romero, A. B.; Thiemens, M. H. Mass-independent Sulfur Isotopic Compositions in Present-day Sulfate Aerosols. *J. Geophys. Res.* **2003**, *108*, No. 4524.
(52) Cao, F.; Zhang, S.-C.; Kawamura, K.; Zhang, Y.-L. Inorganic Markers, Carbonaceous Components and Stable Carbon Isotope from Biomass Burning Aerosols in Northeast China. *Sci. Total Environ.* **2016**, *572*, 1244−1251.
(53) Legrand, M.; Hammer, C.; De Angelis, M.; Savarino, J.; Delmas, R.; Clausen, H.; Johnsen, S. J. Sulfur-containing Species (Methanesulfonate and SO_4) over the Last Climatic Cycle in the Greenland Ice Core Project (Central Greenland) Ice Core. *J. Geophys. Res.: Oceans* **1997**, *102*, 26663−26679.
(54) Calhoun, J. A.; Bates, T. S.; Charlson, R. J. Sulfur Isotope Measurements of Submicrometer Sulfate Aerosol Particles over the Pacific Ocean. *Geophys. Res. Lett.* **1991**, *18*, 1877−1880.
(55) Faloona, I. Sulfur Processing in the Marine Atmospheric Boundary Layer: A Review and Critical Assessment of Modeling Uncertainties. *Atmos. Environ.* **2009**, *43*, 2841−2854.
(56) Li, M.; Zhang, Q.; Kurokawa, J.; Woo, J.-H.; He, K.; Lu, Z.; Ohara, T.; Song, Y.; Streets, D. G.; Carmichael, G. R.; et al. MIX: A Mosaic Asian Anthropogenic Emission Inventory under the International Collaboration Framework of the MICS-Asia and HTAP. *Atmos. Chem. Phys.* **2017**, *17*, 935−963.
(57) Hong, Y.; Zhang, H.; Zhu, Y. Sulfur Isotopic Characteristics of Coal in China and Sulfur Isotopic Fractionation during Coal-Burning Process. *Chin. J. Geochem.* **1993**, *12*, 51−59.
(58) Novák, M.; Jacková, I.; Prechová, E. Temporal Trends in the Isotope Signature of Air-Borne Sulfur in Central Europe. *Environ. Sci. Technol.* **2001**, *35*, 255−260.
(59) Forrest, J.; Newman, L. Sampling and Analysis of Atmospheric Sulfur Compounds for Isotope Ratio Studies. *Atmos. Environ.* **1973**, *7*, 561−573.
(60) Mariotti, A.; Germon, J. C.; Hubert, P.; Kaiser, P.; Letolle, R.; Tardieux, A.; Tardieux, P. Experimental Determination of Nitrogen Kinetic Isotope Fractionation: Some Principles; Illustration for the Denitrification and Nitrification Processes. *Plant Soil* **1981**, *62*, 413−430.
(61) Madronich, S.; Flocke, S. The Role of Solar Radiation in Atmospheric Chemistry. In *Environmental Photochemistry*; Springer, 1999; pp 1−26.

https://dx.doi.org/10.1021/acs.est.9b07150
Environ. Sci. Technol. 2020, 54, 2626−2634

(62) Stockwell, W. R.; Kirchner, F.; Kuhn, M.; Seefeld, S. A New Mechanism for Regional Atmospheric Chemistry Modeling. *J. Geophys. Res.: Atmos.* **1997**, *102*, 25847−25879.
(63) Heard, D. E.; Carpenter, L. J.; Creasey, D. J.; Hopkins, J. R.; Lee, J. D.; Lewis, A. C.; Pilling, M. J.; Seakins, P. W.; Carslaw, N.; Emmerson, K. M. High Levels of the Hydroxyl Radical in the Winter Urban Troposphere. *Geophys. Res. Lett.* **2004**, *31*, No. L18112.
(64) Ren, X.; Brune, W. H.; Mao, J.; Mitchell, M. J.; Lesher, R. L.; Simpas, J. B.; Metcalf, A. R.; Schwab, J. J.; Cai, C.; Li, Y. Behavior of OH and HO_2 in the Winter Atmosphere in New York City. *Atmos. Environ.* **2006**, *40*, 252−263.
(65) Giardina, M.; Buffa, P. A New Approach for Modeling Dry Deposition Velocity of Particles. *Atmos. Environ.* **2018**, *180*, 11−22.
(66) Han, S.; Wu, J.; Zhang, Y.; Cai, Z.; Feng, Y.; Yao, Q.; Li, X.; Liu, Y.; Zhang, M. Characteristics and Formation Mechanism of a Winter Haze−Fog Episode in Tianjin, China. *Atmos. Environ.* **2014**, *98*, 323−330.
(67) Zhang, C.; Wang, L.; Qi, M.; Ma, X.; Zhao, L.; Ji, S.; Wang, Y.; Lu, X.; Wang, Q.; Xu, R.; Ma, Y. Evolution of Key Chemical Components in $PM_{2.5}$ and Potential Formation Mechanisms of Serious Haze Events in Handan, China. *Aerosol Air Qual. Res.* **2018**, *18*, 1545−1557.
(68) Jacob, D. J. Heterogeneous Chemistry and Tropospheric Ozone. *Atmos. Environ.* **2000**, *34*, 2131−2159.
(69) Fu, H.; Wang, X.; Wu, H.; Yin, Y.; Chen, J. Heterogeneous Uptake and Oxidation of SO_2 on Iron Oxides. *J. Phys. Chem. C* **2007**, *111*, 6077−6085.
(70) Adams, J. W.; Rodriguez, D.; Cox, R. A. The Uptake of SO_2 on Saharan Dust: A Flow Tube Study. *Atmos. Chem. Phys.* **2005**, *5*, 2679−2689.
(71) Li, S.; Zhang, G.; Yang, J.; Jia, N. Multi-Source Characteristics of Atmospheric Deposition in Nanjing, China, as Controlled by East Asia Monsoons and Urban Activities. *Pedosphere* **2016**, *26*, 374−385.
(72) Amiri, N.; Ghahremaninezhad, R.; Rempillo, O.; Tokarek, T. W.; Odame-Ankrah, C. A.; Osthoff, H. D.; Norman, A.-L. Stable Sulfur Isotope Measurements to Trace the Fate of SO_2 in the Athabasca Oil Sands Region. *Atmos. Chem. Phys.* **2018**, *18*, 7757−7780.

https://dx.doi.org/10.1021/acs.est.9b07150
Environ. Sci. Technol. 2020, 54, 2626−2634